Validation of a Finite Element Error Estimator

J. O. Dow,* S. A. Harwood,† M. S. Jones,† and I. Stevenson†
University of Colorado, Boulder, Colorado 80309

Several adaptive refinement procedures have been developed to assist designers and analysts in producing finite element meshes with reduced discretization errors. Some of these methods have been criticized for being too circular, i.e., the error measures are too closely related to the finite element results being analyzed. In this work, the smoothed solution against which the finite element stresses are compared is based on a reformulation of the finite difference method that permits irregular meshes and complex boundary conditions to be analyzed. This approach utilizes the finite element displacements, instead of the finite element strains or stresses, to determine a smoothed stress solution, thereby reducing the dependence of the error measures on the finite element results. The errors found by the finite element and the finite difference based methods are found to be nearly identical. This leads to the conclusion that the current finite element error analysis methods are satisfactory for production use and would be a valuable addition to finite element analysis and design packages. Three example problems are presented.

Introduction

THE need for procedures to analyze the accuracy of finite element results and to guide subsequent mesh refinements is well established. The availability of powerful finite element mesh generators and sophisticated graphics output packages allows analysts with little experience to interactively perform complex finite element analyses. In addition, the successful implementation of computer aided design/computer aided manufacturing (CAD/CAM) procedures involves a closed-loop design cycle, which further separates the designer from the analysis. In both situations, the errors introduced by representing a problem with subregions that are not capable of representing the full behavior of the continuum can render the results meaningless. These discretization errors can be identified and controlled by the use of adaptive refinement schemes.

A successful adaptive refinement scheme consists of two procedures: one estimates the errors in the individual finite elements and the other guides the mesh refinement based on the elemental error estimates. A global error estimate, usually consisting of the sum of the individual element error estimates, is used to indicate when to terminate the adaptive refinement procedure.

A procedure for estimating the errors in finite element solutions using error measures based on the finite difference method is developed here.[1] In this approach, the nodal displacements produced by the finite element method are substituted into finite difference operators to give nodal stresses or strains. These stresses or strains are then used to form a continuous or smoothed solution, which is asumed to be closer to the actual result than the discontinuous finite element solution. The smoothed and finite element solutions are then compared using energy measures to compute elemental and global error measures.

Presented as Paper 90-0931 at the AIAA/ASME/ASCE/AHS/ASC 31st Structures, Structural Dynamics and Materials Conference, Long Beach, CA, April 2–4, 1990; received June 25, 1990; revision received Oct. 11, 1990; accepted for publication Oct. 24, 1990.

*Associate Professor, Department of Civil, Environmental, and Architectural Engineering.

†Graduate Research Assistant, Department of Civil, Environmental, and Architectural Engineering.

This finite difference approach is a variant of an existing error estimating procedure. In the existing approach, the smoothed solution is derived from the finite element stress or strain results by an equal energy content[2] or a nodal averaging procedure.[3] These finite element based error estimates have been criticized because the smoothed solutions are found directly from the discontinuous finite element strain resultants to which they are to be compared. The finite difference based error measures are designed to move the computation of the smoothed result one step away from the finite element strain computations. As the results presented here will show, the finite difference and finite element based error measures give approximately the same results. From this, it is concluded that the finite element based approach is satisfactory for production use.

In the Zienkiewicz-Zhu method,[2] the smoothed solution is found by a least squares procedure that minimizes the difference between the strain energies of the smoothed solution and the finite element result while maintaining a constant value for the overall strain energy. The method developed by Dow and Byrd[3,4] averages the stress or strain values at the common nodes of connected elements to form the basis of the smoothed solution. Both finite element based procedures produce nearly identical results. The Dow-Byrd approach has the advantage that it requires less computational effort than the Zienkiewicz-Zhu method. The Dow-Byrd procedure has been extended to plate elements.[4]

The development of the finite difference error analysis procedures is based on a reformulation of the finite difference method, which is outlined in the next three sections.[5,6] Three example problems are then analyzed. The significance of the results is discussed in the concluding section.

Theoretical Development

The measure used to estimate errors in this work is identical to the one developed by Zienkiewicz and Zhu[2] and used by Dow and Byrd.[4] The overall procedure developed here differs from the two finite element based methods only in the way that the smoothed solution is formulated. The Zienkiewicz-Zhu and Dow-Byrd methods utilize strains computed from derivatives of the finite element interpolation functions. The method developed here computes nodal strains with finite difference operators evaluated in terms of the finite element nodal displacements. The polynomial functions used in the determination of these strain quantities differ from those used in the finite element formulation. Because of the nature of the 3×3 finite difference template, a greater number of

nodal displacements are used in the strain computations than are used in the finite element formulation. This approach removes the computation of the smoothed strains one step from the finite element procedure. The nodal strains should be more accurate than the individual finite element results because the strains are computed at a central point using a larger number of nodes than is the case for the finite element computation.

The error measure compares the smoothed solution to the finite element result for each individual element. The absolute values of the differences between the stresses in the two solutions are summed over each individual element. This quantity is weighted by the constitutive properties to produce an energy quantity. This energy measure is written in equation form as,

$$\|e_i\|^2 = \int_{\Omega'} (\sigma^* - \sigma')^T [D]^{-1} (\sigma^* - \sigma') \, d\Omega \qquad (1)$$

where $\|e_i\|$ is the error energy norm in element i, σ^* the smooth stresses, σ' the finite element stresses, D the constitutive matrix, and Ω' the area of element i.

A global error energy norm is computed by summing the individual element error energy norms:

$$|e|^2 = \sum_{i=1}^{\varepsilon} \|e_i\|^2 \qquad (2)$$

A relative global error estimate can be computed by normalizing the global error energy with respect to the estimated total energy contained in the improved solution:

$$\eta = \frac{|e|}{\sqrt{|U'|^2 + |e|^2}} \times 100\% \qquad (3)$$

where $|U'|$ is the energy norm for the finite element solution. The local or elemental error estimates are used to guide the mesh refinement. The global error estimate is used to indicate when to stop the mesh refinement.

Theoretically, this development is straightforward. However, no general procedure for computing finite difference operators for elasticity applications with irregular meshes and complex boundary conditions existed prior to this work.[1,5-7] In fact, the development of the finite element method was spurred by difficulties with boundary conditions in the finite difference method.[8,9] These limitations can be largely overcome through the use of a Taylor series expansion of the displacements in the continuum written in terms of strain gradient notation.

This notation incorporates the knowledge that the displacements in a continuum are due to rigid-body motions and deformations. In short, the derivative coefficients of the Taylor series expansion are expressed as functions of rigid-body terms, strains, and derivatives of strains. For example, the strain gradient term $\gamma_{xy,x}$ quantifies the variation of γ_{xy} in the x direction. The displacements in the x and y directions, u and v, are expressed in strain gradient notation in the Appendix [Eq. (A1)].

The derivation of these displacement expansions is available in papers discussing a variety of applications of this notation. Strain gradient notation has been utilized to evaluate equivalent continuum properties of lattice structures,[10,11] to identify errors in finite elements,[12-14] and to provide an alternative formulation procedure for finite elements.[3,15]

Strain Gradient Based Central Difference Operators

The finite difference method approximates derivatives with difference operators based on a mesh pattern or template. A candidate set of derivatives that a given template is able to approximate can be tentatively identified by comparing the template configuration with a Pascal's triangle. This set is then validated with a check for linear independence.[1]

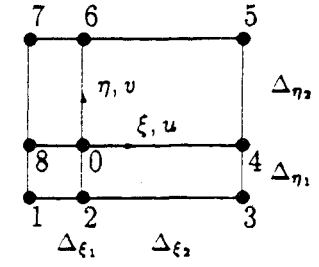

Fig. 1 Difference template.

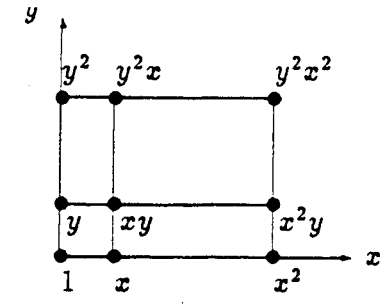

Fig. 2 Displacement variations represented in template.

This development centers around the extensively used 3 × 3 central difference template shown in Fig. 1. The lowest order polynomial and, consequently, the derivatives that this template is capable of modeling are identified using Pascal's triangle, as shown in Fig. 2. When only these polynomial terms are used, the displacement expansions of Eqs. (A1) reduce to Eqs. (A2). In Eqs. (A2), ξ and η are used to emphasize that a local template coordinate system is used. The origin corresponds to the center node of the template.

Equations (A2) are used to form a relationship between the mesh point displacements and the strain gradient quantities. When the expressions for u and v are evaluated by substituting the locations of each mesh point, a set of 18 equations is formed. The 18 × 18 coefficient matrix formed serves to transform the strain gradient quantities to mesh point displacements. The inverse of this transformation gives the difference approximations of the strain gradient quantities as,

$$\{\varepsilon_s\} = [\Phi]^{-1} \{u\} \qquad (4)$$

where

$$\{u\} = \{u_1 v_1 u_2 v_2 u_3 v_3 u_4 v_4 u_5 v_5 u_6 v_6 u_7 v_7 u_8 v_8 u_9 v_9\}^T$$

$$\{\varepsilon_s\} = \{u_{rb} v_{rb} r_{rb} \varepsilon_x \varepsilon_y \gamma_{xy} \varepsilon_{x,x} \varepsilon_{y,x} \gamma_{xy,x} \varepsilon_{x,y} \varepsilon_{y,y} \gamma_{xy,y} \varepsilon_{x,xy} \varepsilon_{x,yy} \varepsilon_{y,xy} \varepsilon_{y,xx} \varepsilon_{x,xyy} \varepsilon_{y,xyy}\}^T$$

and $[\Phi]^{-1}$ is the 18 × 18 transformation matrix. The subscripts on the displacements refer to a template point. The vector $\{\varepsilon_s\}$ contains the 18 strain gradient quantities approximated by the 3 × 3 central difference template.

This approach generalizes the procedures for creating finite difference operators for both regular and irregular meshes. These operators are identical to the standard operators for regular meshes. When the approach is applied to irregular meshes, additional terms are introduced into the finite difference operators. Until now, no formal procedure for formulating irregular meshes has existed.[7] Templates formulated in this manner allow the strains and stresses at the internal nodes of the finite element model to be determined from the finite element displacements. The stresses and strains at boundary nodes are determined from the template formulation described in the following section.

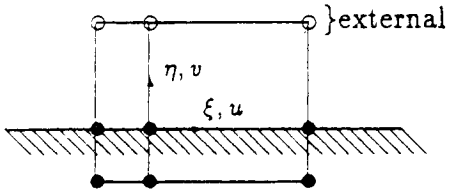

Fig. 3 Boundary template.

Central Difference Boundary Operators

The use of central difference templates on the boundary of the continuum results in nodes that lie outside of the body. A procedure for eliminating these fictitious nodes on a point-by-point basis will now be presented.[6] The information made available by strain gradient notation is used to identify a set of boundary equations that relates the boundary conditions to the template nodal displacements. The degrees of freedom associated with the displacements of the external nodes are used to specify stresses on the continuum that satisfy equilibrium with the prescribed tractions along the boundary.

To illustrate the formulation, the boundary template for a loaded horizontal surface for plane stress, as shown in Fig. 3, will be developed. Here, six degrees of freedom exist outside of the boundary (u and v displacements for three nodes), hence, six independent boundary equations must be identified.

For the boundary shown, the quantities σ_y and τ_{xy} may be specified. Using plane stress constitutive relations to express these tractions in terms of strain gradient quantities, the first two boundary equations are obtained

$$\sigma_y = \frac{E}{1-\nu^2}(\varepsilon_y + \nu\varepsilon_x) \tag{5}$$

$$\tau_{xy} = G\gamma_{xy} \tag{6}$$

where G represents the shear modulus. When the strain gradient quantities represented by the central difference template [Eq. (4)] are examined, the variation of these quantities with respect to x are seen to exist. The first derivatives of σ_y and τ_{xy} provide the next two boundary conditions:

$$\sigma_{y,x} = \frac{E}{1-\nu^2}(\varepsilon_{y,x} + \nu\varepsilon_{x,x}) \tag{7}$$

$$\tau_{xy,x} = G\gamma_{xy,x} \tag{8}$$

When the second derivatives, $\sigma_{y,xx}$ and $\tau_{xy,xx}$, are studied, it is found that the latter term is not available as a boundary equation because the term $\gamma_{xy,xx}$ is not represented in the central difference operator. When the first term is expanded, the result is

$$\sigma_{y,xx} = \frac{E}{1-\nu^2}(\varepsilon_{y,xx} + \nu\varepsilon_{x,xx}) \tag{9}$$

The term $\varepsilon_{x,xx}$ is not represented in the central difference operator. However, it may be obtained from the following compatibility equation of three-dimensional elasticity:

$$\gamma_{xz,xz} = \varepsilon_{x,zz} + \varepsilon_{z,xx} \tag{10}$$

When Eq. (9) is simplified for plane stress, the result is

$$\sigma_{y,xx} = \frac{E}{1-\nu^2}(\varepsilon_{y,xx} - \nu\varepsilon_{y,xx}) = 2G\varepsilon_{y,xx} \tag{11}$$

The final boundary equation is determined from the following three-dimensional compatibility equation:

$$\gamma_{xy,zz} = \gamma_{xz,yz} + \gamma_{yz,xz} - 2\varepsilon_{z,xy} \tag{12}$$

When the conditions of plane stress are introduced into Eq. (12), the equation reduces to

$$\varepsilon_{x,xy} + \varepsilon_{y,xy} = 0 \tag{13}$$

The six boundary equations [Eqs. (5–8), (11), (13)] can be rewritten in matrix form as

$$\begin{Bmatrix} \sigma_y \\ \sigma_{y,x} \\ \sigma_{y,xx} \\ \tau_{xy} \\ \tau_{xy,x} \\ 0 \end{Bmatrix} = \begin{bmatrix} \alpha & \beta & 0 & 0 & 0 & 0 & 0 & 0 & 0 \\ 0 & 0 & \alpha & \beta & 0 & 0 & 0 & 0 & 0 \\ 0 & 0 & 0 & 0 & 2G & 0 & 0 & 0 & 0 \\ 0 & 0 & 0 & 0 & 0 & G & 0 & 0 & 0 \\ 0 & 0 & 0 & 0 & 0 & 0 & G & 0 & 0 \\ 0 & 0 & 0 & 0 & 0 & 0 & 0 & 1 & 1 \end{bmatrix} \begin{Bmatrix} \varepsilon_x \\ \varepsilon_y \\ \varepsilon_{x,x} \\ \varepsilon_{y,x} \\ \varepsilon_{y,xx} \\ \gamma_{xy} \\ \gamma_{xy,x} \\ \varepsilon_{x,xy} \\ \varepsilon_{y,xy} \end{Bmatrix} \tag{14}$$

or

$$\{\sigma,\} = [C]\{\varepsilon,\}$$

where

$$\alpha = E\frac{\nu}{1-\nu^2}$$

$$\beta = E\frac{1}{1-\nu^2}$$

Now that the six boundary equations have been identified, the next step is to form an expression that defines the displacements of the six external degrees of freedom in terms of the boundary tractions and the 12 internal displacements. This is accomplished by substituting a partition of Eq. (4) into Eq. (14) to give

$$\begin{aligned} \{\sigma,\} &= [C][\phi]\{u\} \\ &= [\Theta]\{u\} \\ &= [\Theta_e]\{u_e\} + [\Theta_i]\{u_i\} \end{aligned} \tag{15}$$

where the subscripts e and i refer to the 6 external and 12 internal degrees of freedom, respectively. This equation can be rearranged to give

$$\{u_e\} = [\Theta_e]^{-1}[\{\sigma,\} - [\Theta_i]\{u_i\}] \tag{16}$$

Implicit in this step is the assumption that the matrix $[\Theta_e]$ is nonsingular. This requires that the boundary conditions selected in Eq. (14) represent linearly independent relationships.

Equation (16) specifies the displacements of the external nodes as a function of the internal displacements and the applied surface tractions. With these quantities defined, the full set of stresses at the boundary can be computed on a point-by-point basis. These strains, combined with the interior nodal strains, constitute a nodal smoothed strain solution. From this, a smoothed elemental solution can be computed using the finite element displacement interpolation functions. The error measures are computed from Eqs. (1–3) using these quantities. The global error measure is found by summing the elemental quantities.

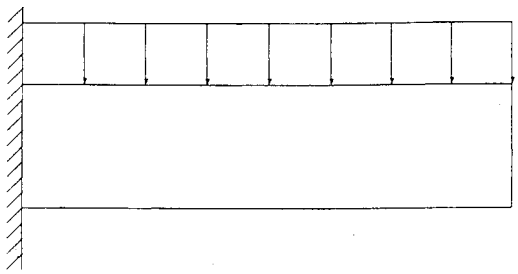

Fig. 4 Cantilever beam with uniform load.

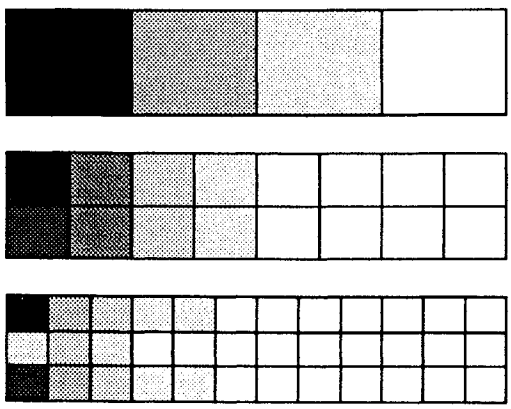

Fig. 5 Finite difference element errors for cantilever problem.

The development for the horizontal surface can be directly extended to a vertical surface. The problems analyzed as examples also requires boundary templates for outside corners, re-entrant corners, sloping surfaces, and fixed boundaries. The formulation of the boundary templates for each of these cases is similar to the development presented here for the horizontal surface. The details are available in Refs. 1 and 6.

The formulation of six boundary conditions for each point on the boundary allows the smoothed stresses on the boundary to be evaluated on a point-by-point basis. However, a set of coupled equations related to each of the external degrees of freedom can be developed that utilize a simpler set of boundary conditions. Equations similar to Eqs. (5) and (6) can be used at each boundary node.[6] If the mesh is irregular, these equations are coupled and a set of equations must be solved simultaneously. The results from either type of analysis are virtually identical. The three representative problems solved next utilize the point-by-point procedure.

Error Analysis Applications

The behavior of the finite difference error estimator is illustrated in this section with three examples. The estimated errors found using both the finite difference and the nodal averaging methods are compared to the errors computed from analytic solutions or from highly refined finite element solutions. All of the problems are modeled with planar four-node quadrilateral elements that have had the parasitic shear terms eliminated. A discussion of the causes and procedures for eliminating parasitic shear can be found in Refs. 3 and 14.

The first example problem is a cantilever beam with a uniformly distributed load along the top (see Fig. 4). The original

Table 1 Results of error analysis for cantilever beam

DOF in mesh	Exact error, %	Finite difference error, %	Nodal averaging error, %
16	30.89	40.37	17.04
48	19.79	21.70	16.59
96	13.50	16.00	13.29

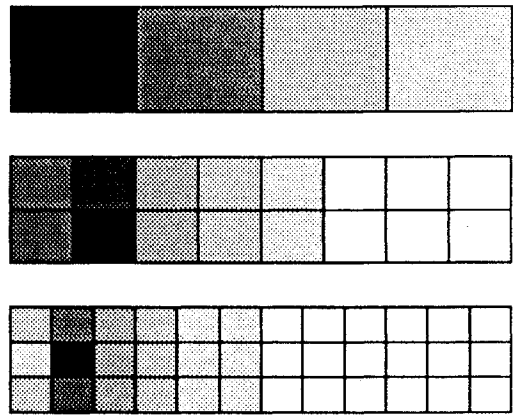

Fig. 6 Nodal averaging element errors for cantilever problem.

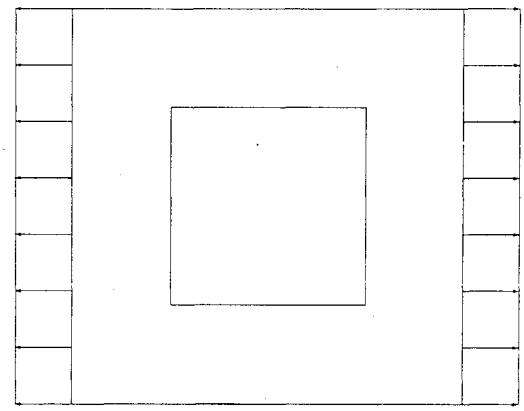

Fig. 7 Plate with square hole in tension.

mesh and the subsequent refinements for the finite difference error analyses are shown in Fig. 5. Figure 6 shows the same information for the nodal averaging error estimator. The three refinements shown in Figs. 5 and 6 are shaded according to the error content of the individual elements. The darker the element, the higher the error content of the element. The shading of the elements is relative only to the elements in a particular refinement; therefore, the magnitude of the errors between refinements cannot be compared in terms of the shading of the elements. The global errors for the three refinements are shown in Table 1. The tabulated data include the actual error, the finite difference error estimates, and the nodal averaging error estimates. The error analysis results indicate that the error estimates are converging to the actual error as the mesh is refined. The finite difference error estimates are larger than the actual errors for all three refinements. The nodal averaging technique is smaller than the actual error in each case.

The second example problem is a square plate with a square hole loaded in tension (see Fig. 7). Because of symmetry, this problem is modeled using a quarter section. The meshes and the relative errors for three successive mesh refinements using the finite difference error estimator are shown in Fig. 8. Figure 9 shows the same information for the nodal averaging error estimator. The results of the error analyses are shown in Table 2.

The error estimators for both the finite difference and the nodal averaging techniques behave in much the same way. They are converging to the actual error from below. For this problem, the nodal averaging error estimators are slightly larger than the finite difference error estimators.

The final example problem is a uniformly loaded tapered beam fixed at both ends (see Fig. 10). The mesh for this problem is irregular, and so the ability of the strain gradient formulation of the finite difference templates to handle ir-

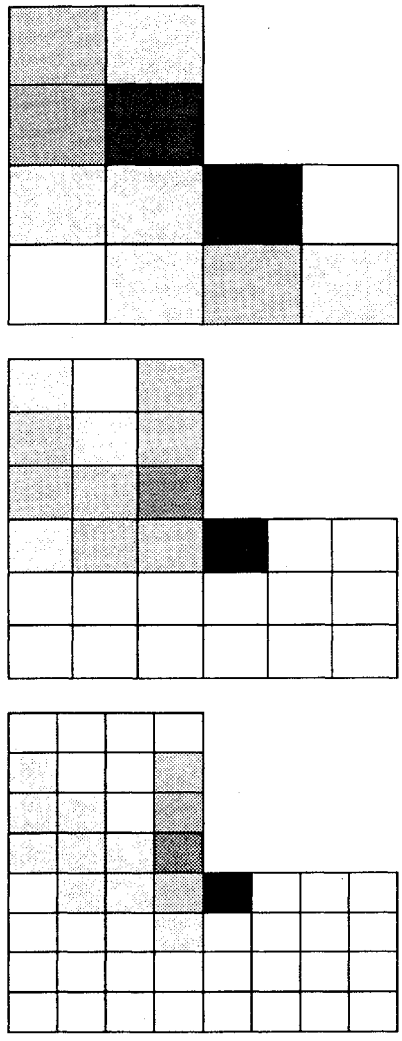

Fig. 8 Finite difference element errors for square hole problem.

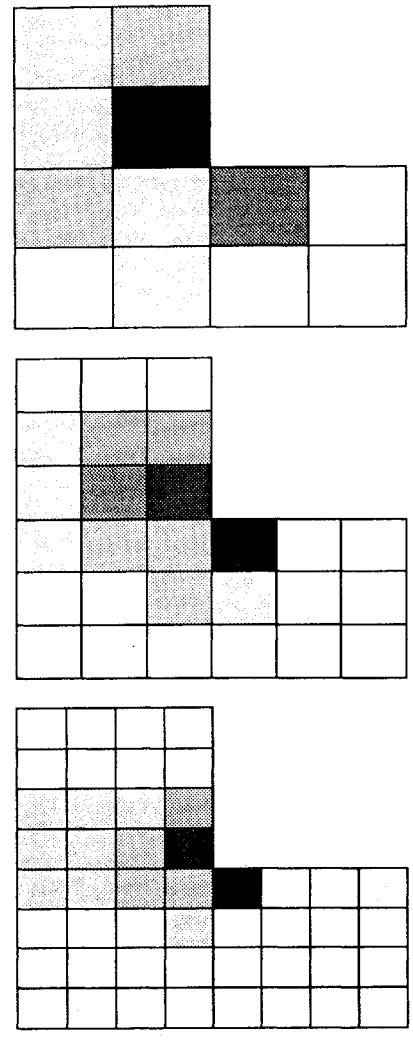

Fig. 9 Nodal averaging element errors for square hole problem.

regular shapes is required for the analysis of this problem. The meshes and the relative errors for three successive mesh refinements using the finite difference and the nodal averaging error estimators are shown in Figs. 11 and 12, respectively. The results of the error analyses are shown in Table 3.

The global error estimates for both methods are similar. They are both converging from below to the actual error as the mesh is refined. For this problem, the nodal averaging error estimators are slightly larger than those for the finite difference method.

The results from the last two problems show that the finite difference and the nodal averaging methods produce nearly identical results. The results of the first example differ markedly from this pattern. In the first example, the finite difference is larger than both the nodal averaging and the actual results. The source of this difference can be identified by examining the elemental errors in the individual problems. Tables 4–6 present the amount of error contained in the element with the largest error.

In the case of example 1, the cantilever beam problem, the maximum error in a single element for the finite difference analysis is substantially larger than the maximum error contained in a single element resulting from the nodal averaging method. A comparison of the coarsest meshes in Figs. 5 and 6 shows that the error is concentrated in the element next to the support. A comparison of the next two refinements shows that the maximum error contained in a single element is much closer for the two methods (see Table 4). When the refined meshes of Fig. 5 are compared to those of Fig. 6, it can be seen that the finite difference and the nodal averaging methods have different patterns of error distribution. In the finite difference analysis, the maximum error is in the row of elements next to the support. In the nodal averaging analysis, the maximum error is contained in the second row of elements from the wall.

A comparison of Figs. 11 and 12 for the tapered beam shows the same pattern of error distribution. The finite difference

Table 2 Results of error analysis for plate with square hole

DOF in mesh	Exact error, %	Finite difference error, %	Nodal averaging error, %
36	33.10	19.75	20.12
70	22.20	14.89	15.99
120	19.80	11.89	13.10

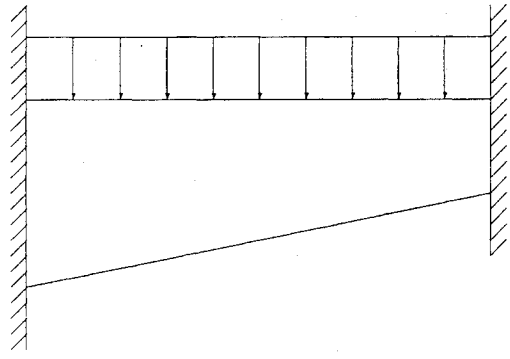

Fig. 10 Fixed-fixed beam with uniform load.

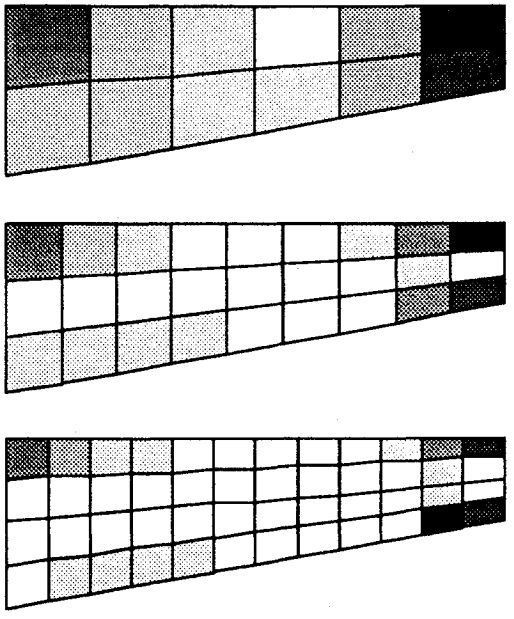

Fig. 11 Finite difference element errors for tapered beam problem.

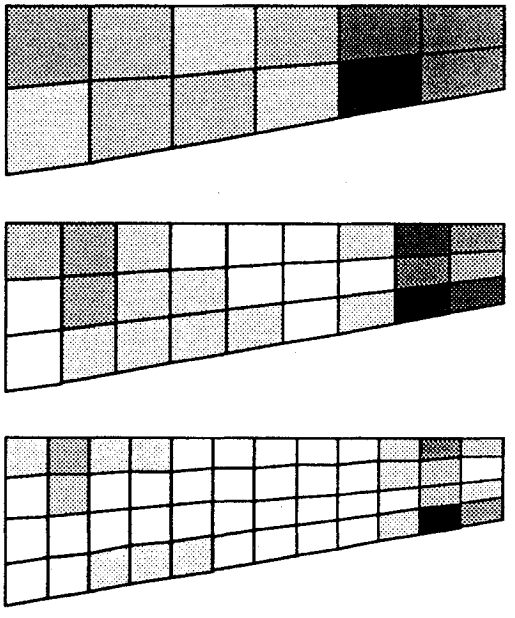

Fig. 12 Nodal averaging element errors for tapered beam problem.

error analysis shows the elements with the larger errors to be adjacent to the supports. This pattern is mirrored in the higher refinements on the left end. The errors found using the nodal averaging technique are one element away from the support. Table 6 shows that the elements with the maximum error contain nearly the same level of error for both cases.

In the second example, no real fixed boundaries exist, and so a discussion of the effects of fixed boundaries would be forced. In this problem, both methods identify the same element as having the largest error in the two higher refinements (see Figs. 8 and 9). The magnitude of the highest element error is approximately the same for each refinement (see Table 5).

The primary difference between the errors estimated by the two methods occurs in the regions adjacent to fixed boundaries. The finite difference based error estimator produces a higher error estimate for the restrained elements than does the procedure based on the smoothed finite element results. A possible cause of this difference is that a larger amount of information is included in the finite difference error estimator for boundary elements. The finite difference approach utilizes displacement information from three interior nodes. The finite element approach includes only the information from one interior point in the strain computation on the boundary because of interelement compatibility. The effect of this difference on the strain representations is currently being studied.

Summary and Concluding Remarks

A finite element error analysis procedure based on a reformulated version of the finite difference method was developed. This procedure is less dependent on the finite element interpolation functions than either the Zienkiewicz-Zhu or the Dow-Byrd approaches. The smoothed solution against which the finite element solution is judged is formed from the more accurate finite element nodal displacements using finite difference operators.

The finite difference and the nodal averaging error procedures produce nearly identical global error and individual error estimates. The similarity in the results indicates that the nodal averaging method is a valid approach for estimating discretization errors in the finite element method. Since the information needed for the nodal averaging error estimator is readily available in many finite element codes, error analysis postprocessors can be easily implemented in these codes. Because of the accuracy of this approach and the guidance it provides for mesh refinement, it is recommended that this approach be made available as a postprocessor where possible.

It is possible that the introduction of these procedures into commercial application may be delayed because of legal implications connected with their designation as error analysis procedures. Because of this, it is suggested that the technically correct name error estimator be relinquished for the legally safer name refinement coefficient. This semantic change may speed the implementation of these procedures for improving

Table 3 Results of error analysis for tapered beam

DOF in mesh	Exact error, %	Finite difference error, %	Nodal averaging error, %
30	40.79	27.78	28.19
64	28.83	22.93	24.11
110	21.69	19.53	20.27

Table 4 Element error results for cantilever beam

DOF in mesh	Finite difference max element error, %	Nodal averaging max element error, %
16	12.36	1.37
48	1.10	0.57
96	0.49	0.26

Table 5 Element error results for plate with square hole

DOF in mesh	Finite difference max element error, %	Nodal averaging max element error, %
16	1.01	1.18
48	0.44	0.47
96	0.25	0.29

Table 6 Element error results for the tapered beam

DOF in mesh	Finite difference max element error, %	Nodal averaging max element error, %
16	1.66	1.50
48	0.89	0.80
96	0.50	0.55

analysis results and bring them to the aid of the designer. However, the questions concerning the legal implications of a name will be resolved elsewhere.

Appendix: Strain Gradient Displacement Approximation

Equations (A1) are the complete fourth-order expansions of the displacement u and v in the x and y directions expressed in strain gradient notation. Equations (A2) are the subsets of Eqs. (A1) that can be represented by a 3×3 finite difference template. In Eqs. (A2), ξ and η are used to emphasize that a local template coordinate system is used. These equations are the following:

$$\begin{aligned} u(x,y) &= [u_{rb}]_0 + [\varepsilon_x]_0 x + [\gamma_{xy}/2 - r_{rb}]_0 y \\ &+ [\varepsilon_{x,x}/2]_0 x^2 + [\varepsilon_{x,y}]_0 xy + [(\gamma_{xy,y} - \varepsilon_{y,x})/2]_0 y^2 \\ &+ [\varepsilon_{x,xx}/6]_0 x^3 + [\varepsilon_{x,xy}/2]_0 x^2 y + [\varepsilon_{x,yy}/2]_0 xy^2 \\ &+ [(\gamma_{xy,yy} - \varepsilon_{y,xy})/6]_0 y^3 + [\varepsilon_{x,xxx}/24]_0 x^4 \\ &+ [\varepsilon_{x,xxy}/6]_0 x^3 y + [\varepsilon_{x,xyy}/4]_0 x^2 y^2 + [\varepsilon_{x,yyy}/6]_0 xy^3 \\ &+ [(\gamma_{xy,yyy} - \varepsilon_{y,xyy})/24]_0 y^4 \end{aligned} \tag{A1a}$$

$$\begin{aligned} v(x,y) &= [v_{rb}]_0 + [\gamma_{xy}/2 + r_{rb}]_0 x + [\varepsilon_y]_0 y \\ &+ [(\gamma_{xy,x} - \varepsilon_{x,y})/2]_0 x^2 + [\varepsilon_{y,x}]_0 xy + [\varepsilon_{y,y}/2]_0 y^2 \\ &+ [(\gamma_{xy,xx} - \varepsilon_{x,xy})/6]_0 x^3 + [\varepsilon_{y,xx}/2]_0 x^2 y + [\varepsilon_{y,xy}/2]_0 xy^2 \\ &+ [\varepsilon_{y,yy}/6]_0 y^3 + [(\gamma_{xy,xxx} - \varepsilon_{x,xxy})/24]_0 x^4 \\ &+ [\varepsilon_{y,xxx}/6]_0 x^3 y + [\varepsilon_{y,xxy}/4]_0 x^2 y^2 + [\varepsilon_{y,xyy}/6]_0 xy^3 \\ &+ [\varepsilon_{y,yyy}/24]_0 y^4 \end{aligned} \tag{A1b}$$

$$\begin{aligned} u(\xi,\eta) &= [u_{rb}]_0 + [\varepsilon_x]_0 \xi + [\gamma_{xy}/2 - r_{rb}]_0 \eta \\ &+ [\varepsilon_{x,x}/2]_0 \xi^2 + [\varepsilon_{x,y}]_0 \xi\eta + [(\gamma_{xy,y} - \varepsilon_{y,x})/2]_0 \eta^2 \\ &+ [\varepsilon_{x,xy}/2]_0 \xi^2\eta + [\varepsilon_{x,yy}/2]_0 \xi\eta^2 + [\varepsilon_{x,xyy}/4]_0 \xi^2\eta^2 \end{aligned} \tag{A2a}$$

$$\begin{aligned} v(\xi,\eta) &= [v_{rb}]_0 + [\gamma_{xy}/2 + r_{rb}]_0 \xi + [\varepsilon_y]_0 \eta \\ &+ [(\gamma_{xy,x} - \varepsilon_{x,y})/2]_0 \xi^2 + [\varepsilon_{y,x}]_0 \xi\eta + [\varepsilon_{y,y}/2]_0 \eta^2 \\ &+ [\varepsilon_{y,xx}/2]_0 \xi^2\eta + [\varepsilon_{y,xy}/2]_0 \xi\eta^2 + [\varepsilon_{y,xxy}/4]_0 \xi^2\eta^2 \end{aligned} \tag{A2b}$$

References

[1]Harwood, S. A., "Finite Element Error Analysis Using the Finite Difference Method," M.S. Thesis, Univ. of Colorado, Boulder, CO, 1989.

[2]Zienkiewicz, O. C., and Zhu, J. Z., "A Simple Error Estimator and Adaptive Procedure for Practical Engineering Analysis," *International Journal for Numerical Methods in Engineering*, Vol. 24, No. 2, 1987, pp. 337–357.

[3]Byrd, D. E., "The Identification and Elimination of Errors in Finite Element Analysis," Ph.D. Dissertation, Univ. of Colorado, Boulder, CO, 1988.

[4]Dow, J. O., and Byrd, D. E., "The Identification and Elimination of Artificial Stiffening in Mindlin Plate Elements," *Proceedings of the 30th AIAA/ASME/ASCE/AHS/ASC Structures, Structural Dynamics, and Materials Conference*, AIAA, Washington, DC, April 1989, pp. 2208–2216.

[5]Dow, J. O., Jones, M. S., and Harwood, S. A., "A Generalized Finite Difference Method for Solid Mechanics," *International Journal of Numerical Methods for Partial Differential Equations*, Vol. 6, No. 2, 1990, pp. 137–152.

[6]Dow, J. O., Jones, M. S., and Harwood, S. A., "A New Approach to Boundary Modeling for Finite Difference Applications in Solid Mechanics," *International Journal for Numerical Methods in Engineering*, Vol. 30, No. 1, 1990, pp. 99–113.

[7]Perrone, N., and Kao, R., "A General Finite Difference Method for Arbitrary Meshes," *Computers and Structures*, Vol. 5, No. 1, 1975, pp. 45–58.

[8]Thomasset, F., *Implementation of Finite Element Methods for Navier-Stokes Equations*, Springer-Verlag, New York, 1981.

[9]Zienkiewicz, O. C., "The Finite Element Method: From Intuition to Generality," *Applied Mechanics Review*, Vol. 23, No. 3, 1970, pp. 249–256.

[10]Dow, J. O., Feng, C. C., and Bodley, C. S., "An Equivalent Continuum Representation of Structures Composed of Repeated Elements," *AIAA Journal*, Vol. 23, No. 10, 1985, pp. 1564–1569.

[11]Dow, J. O., and Huyer, S. A., "Continuum Models of Space Station Structures," *ASCE Journal of Aerospace Engineering*, Vol. 2, No. 4, 1989, pp. 220–237.

[12]Dow, J. O., Ho, T. H., and Cabiness, H. D., "A Generalized Finite Element Evaluation Procedure," *ASCE Journal of Structural Engineering*, Vol. 111, No. 2, 1985, pp. 435–452.

[13]Dow, J. O., and Byrd, D. E., "The Identification and Elimination of Artificial Stiffening Errors in Finite Elements," *International Journal for Numerical Methods in Engineering*, Vol. 26, March 1988, pp. 743–762.

[14]Dow, J. O., and Byrd, D. E., "Error Estimation Procedure for Plate Bending Elements," *AIAA Journal*, Vol. 23, No. 4, 1990, pp. 685–693.

[15]Dow, J. O., Cabiness, H. D., and Ho, T. H., "A Linear Strain Element with Curved Edges," *ASCE Journal of Structural Engineering*, Vol. 112, No. 4, 1986, pp. 692–708.